2013

Comparison of the Lenstar Optical Biometer and A-scan Ultrasonography to Measure Ocular Components

Drew W. Gann
University of Alabama at Birmingham

COMPARISON OF THE LENSTAR OPTICAL BIOMETER AND A-SCAN ULTRASONOGRAPHY TO MEASURE OCULAR COMPONENTS

by

DREW GANN

THOMAS T. NORTON, CHAIR
ROBERT ANGUS
JOHN T. SIEGWART

A THESIS

Submitted to the graduate faculty of The University of Alabama at Birmingham,
in partial fulfillment of the requirements for the degree of
Master of Science

BIRMINGHAM, ALABAMA

2013

COMPARISON OF THE LENSTAR OPTICAL BIOMETER AND A-SCAN ULTRASONOGRAPHY TO MEASURE OCULAR COMPONENTS

DREW GANN

BIOLOGY 5TH YEAR MASTER'S PROGRAM

ABSTRACT

The purpose of this study was to compare ocular component dimensions and treated minus control eye differences measured with the Lenstar optical biometer to those measured with A-scan ultrasound in the tree shrew model of refractive development and induced myopia.

A-scan ultrasonographic measures (A-scan) were taken with a 15 MHz focused pulser/receiver and compared with measures made with the Lenstar LS900 optical biometer (Haag-Streit, Basel, Switzerland). Anterior segment depth (ASD), lens thickness (LT), vitreous chamber depth (VCD), and axial length (AL) were measured in treated eyes (30), fellow control eyes (30), and normal eyes (86) in tree shrews (n=146), between 10 days after eye opening (days of visual experience [DVE]) and 1973 DVE. Lenstar VCD analyses were made using the retinal cursors. Treated vs. control eye differences were measured (n=60) in eyes made hyperopic or myopic by treatment with a monocular lens or by form deprivation.

The A-scan measures and Lenstar measures were generally comparable (3.5% smaller) when the Lenstar was compared to the A-scan excluding vitreous chamber, which was substantially smaller (23%). If either the lens cursors or the retinal cursors (international software version) were used to measure vitreous chamber depth, Lenstar

values were very similar (3.4% smaller than A-scan). All components (ASD, LT, VCD, and AL) were found to be highly correlated with a consistent offset (t-test; $p < 0.05$). Comparing treated vs. control eye differences of myopic (elongated) and hyperopic (shorter) eyes after monocular treatment showed a significant difference in VCD and AL (t-test; $p < 0.05$). The difference in vitreous chamber depth per diopter difference was 27.2 μm/D for A-scan and 26.1 μm/D for Lenstar. The correlation coefficients were consistently larger for the Lenstar than the A-scan. The slopes between the two systems were not significantly different.

Using the standard cursors, the Lenstar substantially underestimates vitreous chamber depth in tree shrews compared with A-scan. Using the retinal (or lens) cursors to measure the vitreous chamber gives comparable results. The treated vs. control eye vitreous chamber differences (retinal cursors) in monocularly treated animals are very similar. In tree shrews, the Lenstar LS900 can be used in place of A-scan ultrasonography and has the advantage that it can be used in awake animals.

Key Words: Ocular components, Animal models/studies, Refraction, Lenstar optical biometer

DEDICATION

I would like to dedicate this thesis to the three closest people in my life, my father, Danny Gann; my mother, Diann Gann; and my partner, Miranda Hodges. All three of you have contributed to this thesis in more ways than anyone will ever know. Dad, you helped me at my lowest point and taught me countless valuable lessons in life that I could not have learned anywhere else. Mom, you helped me understand that if I worked hard, many opportunities would come my way in helping me to become an optometrist. Lastly, Miranda you were there with me through it all encouraging me every step of the way. Without your constant daily support, I would not be where I am today. I would like to thank each of you for your support and advice. You have each made countless sacrifices in order for me to concentrate on school and this project. I love you all and would like to thank you for everything.

ACKNOWLEDGMENTS

I would like to thank Dr. Thomas Norton for assisting me in providing the idea for this project and for his constant support and knowledge throughout this project. I would also like to thank Dr. John Siegwart, Jr. for providing valuable insight into both the Lenstar and A-scan systems and for providing me with the resources to build my knowledge. I would also like to thank him for teaching me the proper techniques for measuring the animals on these machines. Without this knowledge, this project would not be possible. I would also like to thank Dr. Michael Frost who taught me the basics of what a scientific article is built upon, the mindset of a scientist, and how to properly take criticism and build upon it. Lastly, I would like to thank Dr. Robert Angus for showing me the correct statistical analysis for this project, providing me with the knowledge and background on correct statistical tests, and for providing valuable spreadsheets to perform statistical tests that saved me countless hours. Without all of you, this study would not have been possible.

TABLE OF CONTENTS

Page

LIST OF TABLES

Tables *Page*

LIST OF FIGURES

LIST OF ABBREVIATIONS

AL	axial length
ASD	anterior segment depth
DVE	days of visual experience
LT	lens thickness
SD	standard deviation
VCD	vitreous chamber depth

CHAPTER 1

INTRODUCTION

Myopia, or near-sightedness, is a condition in which visual images are focused in front of the retina. Myopia currently affects approximately 20 - 40% of the U.S. and European populations, with an even higher prevalence in East Asia (Vitale et al., 2009; Fledelius, 1988; Goh & Lam, 1994). Treatment of this refractive error can become a financial burden. In 1995, 13.2 billon dollars were reportedly spent in the United States on frames, lenses, and contact lenses (Sheedy, 1996). Severe (pathological) myopia is a major cause of blindness (Curtin, 1985). Even low myopia raises the risks of blinding eye diseases (Burton, 1989). Even with a considerable amount of new knowledge gained this century, no effective treatments have been yet developed to slow myopia progression or to prevent myopia. Myopia has become an important topic in vision research and clinical fields but even today the causes of juvenile-onset myopia still remain a mystery. Understanding the mechanism of myopia development is crucial in the advancement of treatment or prevention of this refractive disorder.

Parts of the Eye and Refractive States of the Eye

The eye consists of various ocular components (Figure 1). In order to see clearly, images must be focused on the retina. Light has to pass through the cornea, anterior chamber, lens, vitreous chamber, and be focused on the retina. The photoreceptors in the retina detect light and convert it to chemical and electrical impulses that are sent to the visual centers of the brain. For this project, the following components are of central interest: cornea, anterior chamber, (together, called the anterior segment), lens, vitreous, retina, and choroid. The cornea is the clear front of the eye and along with the lens refracts light to form a focal plane where images are in focus. While the cornea contributes most of the eye's focusing power, its focus is fixed. The anterior chamber is the fluid filled space that separates the cornea from the lens. It is filled with aqueous humor. The lens is a transparent, bi-convex structure that also refracts light. The lens can change shape in order to change its focal power. This allows the eye to focus objects at various distances. The vitreous chamber occupies around two-thirds of the human eye's volume and contains the vitreous humor which is a transparent gel that helps give the eye its shape and form. The retina is the photosensitive layer of the eye. Once light is absorbed by the retinal photoreceptors, a complicated series of chemical cascades occurs. These cascades trigger nerve impulses that travel up the axons of the optic nerve and into the visual portions of the brain. The choroid is the vascular layer of the eye that lies between the retina and sclera; it contains blood vessels, connective tissue, and provides oxygen and eliminates waste.

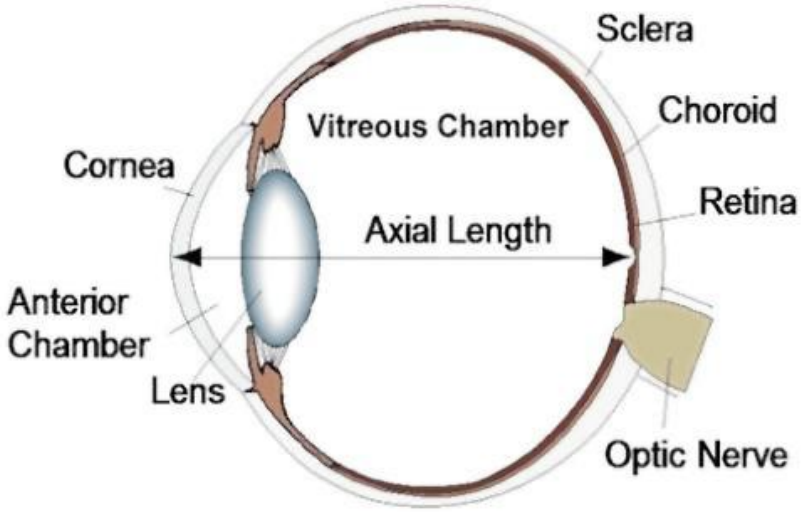

Figure 1. Schematic of the eye. The parts of the eye that are of central concern in this article are the anterior chamber, lens, vitreous chamber, retina, choroid, and overall axial length. All of these components work together to help individuals see clearly. Source: Norton lab image library.

There are three primary refractive states of the eye: emmetropia, myopia, and hyperopia. Emmetropia occurs when light rays enter the eye and are focused on the photoreceptors of the retina. An emmetropic eye is one that sees clearly at distance because the axial length places the retina at the focal plane where the light is focused by the lens and cornea. In hyperopia, the axial length is short, so the retina is in front of the focal plane and images are out of focus on the retina. In myopia, the axial length has become too long, relative to the focal plane, so that the retina is behind the focal plane. Juvenile-onset myopia typically is caused by an increase in axial elongation that moves the retina behind the focal plane.

The Emmetropization Mechanism

Until animal models were developed, it was not known why so many people become emmetropic. An emmetropization mechanism has been shown to exist in a variety of animals including monkeys, tree shrews, and chickens (Wiesel & Raviola, 1977; Sherman et al., 1977; Wallman et al., 1978). The existence of an emmetropization mechanism first became apparent when the functioning of the mechanism was disrupted in animals in 1977 using, first monkeys (Wiesel & Raviola, 1977), and then tree shrews (Sherman et al., 1977). It was found that if infantile animal eyes were deprived of clear images, the axial length increased, moving the retina past the focal plane, causing a myopic eye. As described below, this mechanism normally uses refractive error to guide axial elongation rate of the juvenile eye in order to match the retinal location to focal plane of the eye (Sherman et al., 1977; Wiesel & Raviola, 1977; Wallman et al., 1978).

The Tree Shrew Animal Model

This study investigated the ocular component dimensions in tree shrews (Figure 2), a mammalian species with excellent vision for animals of its size. Tree shrews offer many advantages for studying experimentally-induced myopia. Tree shrews are closely related to primates (Campbell, 1966), increasing the likelihood of a shared mechanism with humans. The tree shrew has good responses to both form deprivation and other environmental manipulations. They breed rapidly, generally producing 2-3 pups per litter. They also mature rapidly, allowing for a reasonable number of animals so that statistical analyses with reasonable power can be accomplished in a short period (Norton and McBrien, 1992).

Figure 2. Tree shrew (*Tupaia glis belangeri).* Photo of species used in the lab to induce myopia or hyperopia. Photo from Norton lab image library.

Tree shrews are born with their eyes closed; their eyes open typically around 21 days after birth (Marsh-Tootle & Norton, 1989; Norton & McBrien, 1992). The day of eye opening for tree shrews is defined as the first day of visual experience (DVE). When eyes first open, they are typically very hyperopic (approximately +25D). During the first 15 DVE, this normal hyperopia decreases dramatically to around +2 D (Norton and McBrien, 1992).

Manipulating the Emmetropization Mechanism in Tree Shrews

In order to test the ability of the emmetropization mechanism to match the retinal position to the focal plane and to examine the underlying mechanisms, lenses are used to alter the refractive state of the eye. This in turn causes the emmetropization mechanism to

adjust the axial length of the eye. The three paradigms used to study the emmetropization mechanism include: minus lens wear, form deprivation, and plus lens wear.

If a monocular minus (concave) lens is held in front of an eye with a goggle frame, it shifts the focal plane away from the cornea. This causes the eye to be hyperopic compared to the original condition, and to that of the fellow, untreated eye. In a juvenile, tree shrew that is still growing, the lens-wearing eye responds to this refractive stimulus by activating the emmetropization mechanism and causing an increase in the axial length of the eye. The increase in axial length is primarily an increase in the vitreous chamber depth. This increase moves the retina to the shifted focal plane and eliminates the induced refractive error (Figure 3, blue triangles), returning the eye back to an emmetropic state while wearing the lens (Siegwart and Norton, 1993). However, when the lens is removed, the eye is myopic because the focal plane is now in front of the retina (Figure 3, green triangles). This situation is referred to as lens-induced myopia because the lens instigated the initial increased growth of the vitreous chamber. If the lens is removed, the myopic refractive error activates the emmetropization mechanism in the growing animal and causes a slowed elongation rate. The optics, cornea and lens, continue to develop (lose optical power) and eventually the focal plane “catches up” to the initially increased axial length (Amedo et al. 2012). This is defined as recovery (Figure 3, orange triangles).

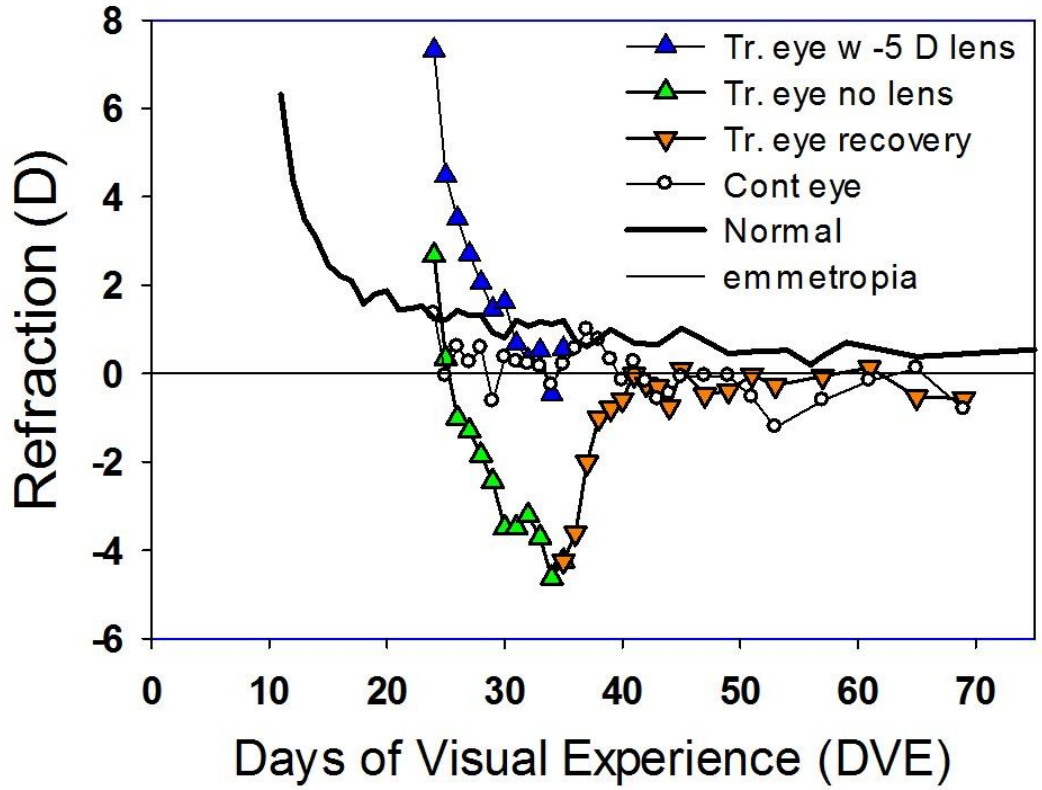

Figure 3. Minus lens development and recovery. The blue triangles show an eye, wearing a minus lens, responding to the lens by increasing the axial length. This reduces the lens-induced hyperopia until it reaches emmetropia (0 D on the Y-axis). The green triangles show the same effect without the lens in place. Thus, the eye develops lens-induced myopia. The orange triangles show the pattern of recovery once lens wear is discontinued. This figure shows how it is possible to manipulate the tree shrew eye to study the emmetropization mechanism to better understand myopia. Figure from Norton lab image library.

Form deprivation was originally performed using eyelid closure and was found to produce myopia in various animals including monkeys, chickens, and tree shrews (Wiesel & Raviola, 1977; Sherman et al., 1977; Wallman et al., 1978). Form deprivation, like minus lens wear, produces axial elongation and myopia. For the last 20 years, translucent diffusers have been used instead of eyelid closure. Diffusers elimate clear images and produce a constant blurred/distorted image on the retina but do not greatly

reduce retinal illuminance. This is very similar to the negative lens wear except the eye can never perceive a clear image, the emmetropization mechanisim continues enlongating the eye because it cannot detect that emmetropia has been restored, as is the case with minus lens wear (Siegwart and Norton, 1998; Norton et al., 2010).

The third method used to study the emmetropization mechanism is plus lens treatment. Placing the plus lens in front of an emmetropic eye initially shifts the focal plane in front of the retina creating a myopic refractive state. The eyes of very young (11 DVE) tree shrews respond to the plus lens treatment by slowing their axial elongation rate so that the eye becomes emmetropic while wearing the plus lens (Figure 4, blue circles). If the lens is removed, the eye is hyperopic (open symbols in Figure 4) (Siegwart, Jr. & Norton, 2010).

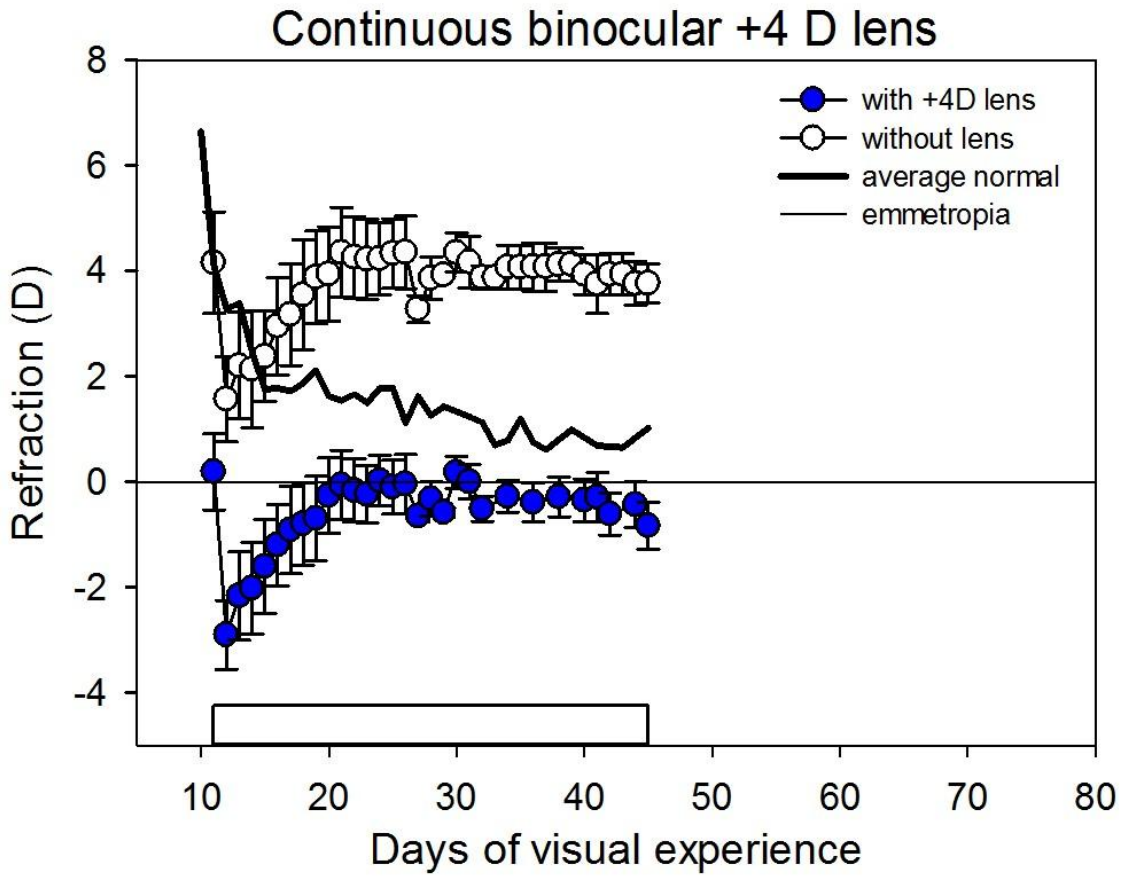

Figure 4. Continuous binocular plus lens wear. The blue circles show the average refraction of the left and right eyes. The eyes initially become myopic after plus lens wear begins followed by the slowed growth of the axial length so that the eyes eventually return to emmetropia while wearing the lenses. The open symbols show the same measurement without the lenses in place. Figure from Norton lab image library.

Ocular Component Measurements

A-scan ultrasound was developed for use in vision research to solve a fundamental problem: how to take measurements of ocular component dimensions over time without damaging the eyes. Before A-scan, the only way to measure ocular component dimensions was to use a caliper to directly measure the ocular components**.** In order to do this, the eye had to be removed from the head; to measure components such as corneal or lens thickness, the eye had to be dissected so that these could be measured. This was not

satisfactory if one wanted to make repeated measures over time, in order to learn what components change during normal development, or when myopia or hyperopia develops, because measures could only be made once per animal. The development of A-scan allowed non-invasive measurements to be made repeatedly and allowed examination of changes in the eye over time. Using A-scan, it has been found that the changes in myopic animal models are similar in to those in myopic human eyes. For myopic eyes, both human and tree shrew, the A-scan showed that vitreous chamber enlargement produces the myopia; while other dimensions change to a much lesser degree.

The A-scan system measures anterior segment depth (ASD), lens thickness (LT), vitreous chamber depth (VCD), and axial length (AL) and has been a crucial piece of equipment for ocular measurement. It uses high frequency sound, reflected off of boundaries between regions of differing density, to measure ocular components and provides the ability to follow normal development and to compare a 'treated' (myopic or hyperopic) eye to a control. However, it also has disadvantages. Because ultrasound does not conduct well through air, the A-scan probe has to contact the cornea in order to make measurements. For most animal models, measurements have to be made while the animals are anesthetized because the animals will not tolerate the probe approaching and contacting the cornea. Repeated anesthesia can have negative consequences such as the possibility of affecting the animal's growth and health. It is unwise to take daily measures because daily anesthesia can affect the health of the animals and may alter ocular development.

Although A-scan ultrasound is still considered the "gold standard" for animal and human myopia studies, a new instrument has recently become available that offers a number of advantages. The Lenstar optical biometer (Haag-Streit) was released for sale

in 2008 and uses light instead of sound to measure ocular dimensions. This machine was developed for human eyes to help clinicians select the correct power of intraocular lenses during cataract surgery. Like the A-scan, the Lenstar creates waveforms that indicate the location of surfaces within the eye. By measuring eyes repeatedly in juvenile animals, one can examine the growth of ocular components; by examining both eyes, one can determine the differences in ocular components between a treated eye and a control eye. A benefit of the Lenstar is that it does not require direct contact to the eye so animals need not be anesthetized. This allows daily measures and eliminates any chance for hindering growth or health due to anesthesia. The Lenstar also is able to measure ocular components that A-scan cannot measure including central corneal thickness, anterior chamber depth, retinal thickness, and even choroidal thickness.

A-Scan Ultrasound Biometry – Principles of Operation

A-scan systems use a type of "pulse-echo" sound waves similar to those found in sonar. This involves a short burst of ultrasonic energy generated by a piezoelectric transducer. The ultrasound waves undergo a partial reflection off of surfaces that have greater or lower density, return to the transducer (which also serves as a microphone to receive the ultrasound), and are displayed on an oscilloscope or monitor screen with time on the X-axis and waveform amplitude on the Y-axis (Figure 5). The horizontal axis represents elapsed time for the ultrasound to move from the transducer to the reflective surfaces and back to the transducer; reflections from more distant surfaces take longer to return relative to nearer surfaces.

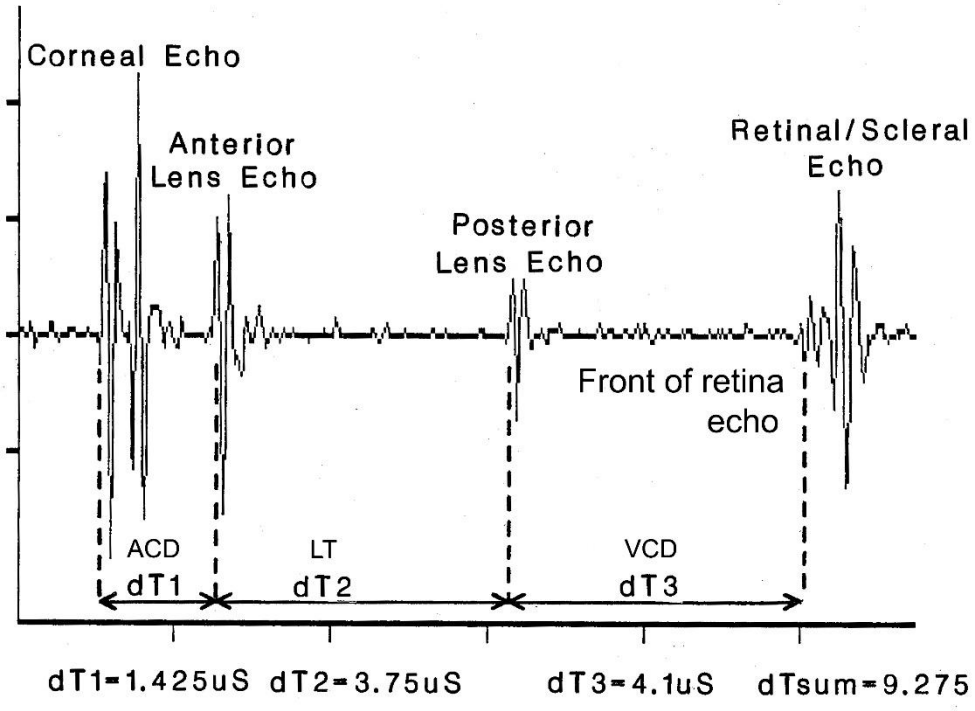

Figure 5. Sample A-scan waveform. This waveform shows the position of the corneal front-surface echo, front and back lens echoes, and retinal/scleral echo. The distances between the components are listed below the scan as dT1 (ACD), dT2 (LT), and dT3 (VCD). Figure from Norton lab image library.

The higher the frequency of the transducer, the better the resolution observed. Increasing the frequency of the transducer leads to increased axial resolution and accuracy. The increase in accuracy is due to the measurement of the first quarter cycle of each echo (fraction of time in which voltage pulse rises to a maximum) (Coleman et al, 1977). However, higher frequencies do not penetrate as deeply into ocular tissues, which places a practical limit on the useful frequencies. In this laboratory, a 15 MHz frequency is used.

A-scan Principle - How Does it Work in the Eye?

The axial ultrasonogram is obtained by aligning the ultrasound beam with the eye's optical axis so that echoes to be obtained from each of the optical surfaces of the

eye. Figure 6 illustrates the difference between a control eye and a treated (myopic) eye. As the figure shows, the vitreous chamber is primarily what is increasing as the eye becomes myopic.

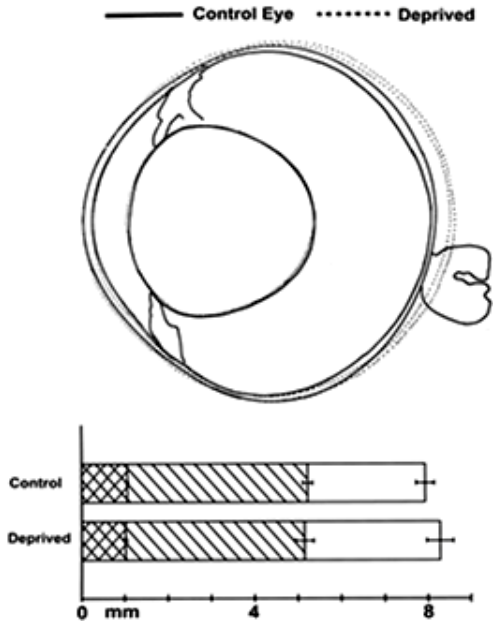

Figure 6. Distances measured between the ocular components with an A-scan. This figure shows tracings of the ocular components of histological sections through the middle of a control and a myopic tree shrew eye. The solid line traces the outline of the normal eye and the dotted line shows the treated eye. The bottom rulers illustrate results of A-scan measures of the two eyes. It can be noted that the vitreous chamber depth is what is increased in the myopic eye. The A-scan analysis of tree shrews was one of the first techniques that showed the vitreous chamber increasing as the eye grew larger and more myopic (Modified from Norton lab library).

Lenstar - Principles of Operation

The operation of the Lenstar is similar to ultrasonography except that light is used rather than sound waves. With light, optical measurement can be performed without physical contact to the eye (Puliafito et al, 1996). The A-scan uses conduction velocities to calculate distances while the Lenstar uses refractive indices to calculate distances. The

principal difference between ultrasonic and optical imaging is speed. Since distances within the eye are measured by the time delay of reflected sound or light waves and light rays travel much faster than sound, this implies that measurements using light require a faster time resolution. The Lenstar uses a principle known as Ocular Low-Coherence Reflectometry (OCLR). Because the Lenstar technology is proprietary, it was difficult to find information about exactly how it works. However information was readily available about the principle of Ocular Coherence Tomography (OCT), which is similar to OCLR. The main difference between these techniques is fairly simple. OCLR takes a single measurement along one axis (often called an A-scan) and OCT uses several scans to create a 2-D section (a B-scan). In its simplest form, OCT is multiple OCLR scans. Thus, the rest of this section describes OCT.

Optical Coherence Tomography utilizes low-coherence interferometry to perform high resolution range measurements and imaging. In order to perform these high resolution structural measurements, it is necessary to use an optical instrument which compares one optical beam to another. This measurement is performed by an interferometer (Puliafito et al, 1996).

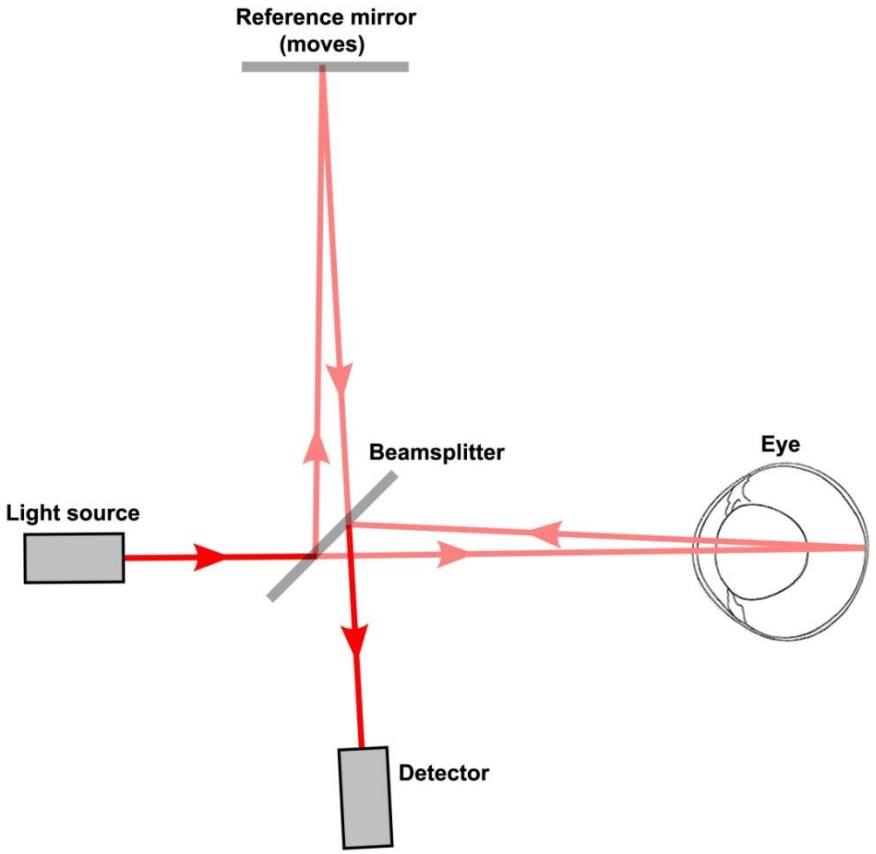

Figure 7. The basic principle behind the Lenstar uses a technique known as low-coherence interferometry. As shown here, the light source emits a beam which is split into two separate beams by the beam splitter. The transmitted beam goes into the eye and reflects off of different tissues at different time delays. These reflected waves combine with the other beam that is reflected from a moving mirror with a known spatial position. These beams combine to produce interference. The type of interference observed depends on the frequency of the two beams. This technique, even though it is complicated, allows greater resolution than that of the A-scan system.

The interferometer uses an optical beam from a laser which emits short optical pulses onto a partially reflective mirror called an optical beam-splitter (Figure 7). The beam-splitter splits the light into two identical beams. One beam (the measurement beam) is directed into the eye and reflects from the intraocular structures where there are differences in refractive index, just as A-scan reflects off of these structures. The reflected measurement beam consists of multiple wave echoes which give information about loca-

tion of the structures. The other half of the split beam, the reference beam, reflects from a mirror that moves and has a known spatial position at any moment. The reflected reference beam then travels back to the mirror where it then combines with the structurally reflected beam. The measurement beam is reflected from the structures with different time delays according to the location of the structure. The light in the reference beam is reflected from the reference mirror at a variable distance in order to produce a time delay. The reflected wave from the measurement beam and the reference beam combine to produce constructive interference only at the locations where the measurement beam has reflected off of an optical surface; the amplitude of the interference signal is measured by a photodetector. The position of the reference mirror is known to the instrument, so that time delays of light echo from the ocular structures can be measured and converted into distance. Figure 8 provides an example of a Lenstar waveform. The top scan is an example of a treated eye (myopic eye), while the bottom is the control eye in the same animal.

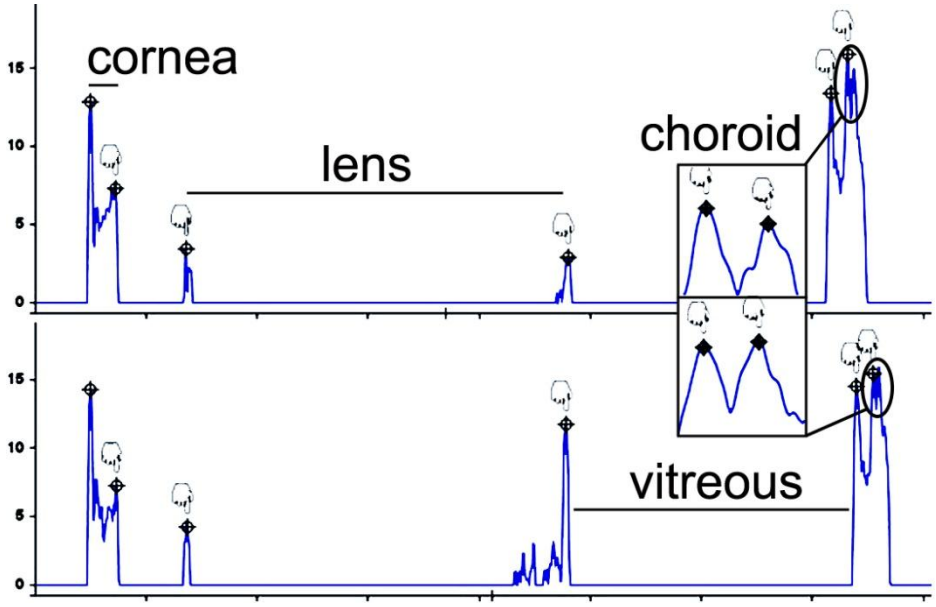

Figure 8. This shows an example waveform from the Lenstar with the top being a treated eye and the bottom being a control eye. It clearly shows the corneal thickness defined as the first two cursors followed by the lens and the vitreous. The retina is indicated by the last two points. The choroid is located where the last cursor is located and is magnified in the images shown for clarity. Image from Norton lab image library.

If this new technology is to be used instead of A-scan, it is necessary to learn how measures of ocular component dimensions made with the Lenstar compare with the A-scan, which has been the accepted system for decades. Are the measures of each ocular component similar? If they differ, is this difference consistent when eyes of differing size are measured? Will the Lenstar show a similar enlargement of the ocular components to the A-scan during normal growth, enlargement of the vitreous chamber in myopic eyes and smaller vitreous chamber in hyperopic eyes? The Lenstar was developed for clinical measures of human eyes but is able to make measures in tree shrew eyes that are around one third of the length of human eyes. How will the measurements made by this system respond to these smaller eyes? The Lenstar must use refractive indices for the ocular

components that are appropriate for humans but may not be appropriate for tree shrews. Will treated vs. control eye differences be similar with both systems?

To answer these questions, this study had two primary aims. Aim 1 compared ocular dimensions between both the A-scan and the Lenstar in normal and control eyes of various ages. Because eyes enlarge with age in young animals, this provides an estimate of whether the two systems give comparable results with different eye sizes. If a significant difference is found between the two systems, a correction factor will be calculated in order to make the differences comparable.

Aim 2 focused on the differences between the treated and control eyes, comparing these differences measured with the A-scan and the Lenstar, treated vs. control eye differences will be analyzed to see if these values are comparable between the two systems.

CHAPTER 2

MATERIALS AND METHODS

Animal Subjects

Measurements of ocular components were made with both A-scan and Lenstar on tree shrews (*Tupaia glis belangeri*) that were born after 11/11/2007. The tree shrews were raised by their mothers in the breeding colony at the University of Alabama at Birmingham. The colony was under a 14h light/10h dark cycle controlled by an automatic timing system. The treatments were in accordance with the ARVO statement for Care and Use of Animals in Ophthalmic and Vision Research and were approved by the Institutional Animal Care and Use Committee.

A total of 146 eyes were measured including 86 normal eyes, 30 untreated control eyes in animals that had the other eye treated with a monocular -5D lens, +5D lens, or diffuser; thus, there were 30 treated eyes. For animals that received monocular treatment, the treated eye was randomly determined. Normal eyes were those that had not yet begun any lens or diffuser wear; most were pre-treatment measures at the start of treatment. For analysis purposes, the control eyes were grouped with the normal eyes because numerous studies in this lab have found that the refractions of the control eyes do not differ significantly from normal (Siegwart and Norton, 1993). One animal included with the normal group was measured at 1937 DVE, after recovering for over 5 years from brief binocular +5 D lens wear. Its refractions appeared normal at this point so it was included in the

normal group. Measurements were made between 10 days after eye opening (days of visual experience [DVE]) and 1937 DVE (median = 23.5 DVE). The range of the ages at which the animals were measured was: normal and control, 10 to 1927 DVE; treated, 10 to 47 DVE).

Because the objective of the normal eye study was to compare A-scan and Lenstar measures on as many eyes as possible, the two eyes of normal animals were measured with both instruments and the eyes were considered individually in the normal eye analysis. During treatment, the animals wore a binocular goggle in which the monocular treatment lens (minus lens, plus lens, or diffuser) was held (Figure 9).

Measurements made by both the A-scan and Lenstar were rarely performed on the same day. A comparison was performed on all the measured eyes and a range of no greater than three days was found to be the largest available difference between the two systems. A cutoff of three days maximum between A-scan and Lenstar measures was utilized for all animal groups. This cutoff was utilized because this was the common spread of days between which the A-scan measures were performed and the Lenstar measures were performed. For analysis, the age of measurement was the average of the two different ages of measurement.

Figure 9. Image shows a juvenile tree shrew that was undergoing lens treatment. The pedestal had been installed and was holding the goggle system. The left eye is the control eye while the right is receiving treatment with a lens. Depending on the type of lens the animal received the emmetropization mechanism could cause it to become myopic or hyperopic. The Lenstar and A-scan measures were used to determine how the ocular components changed in the treated eyes. Photo from Norton lab image library.

Pedestal Installation

In order to hold a lens or diffuser in place in front of an eye, a dental acrylic pedestal was attached to the skull of all animals in this study using published procedures (Siegwart & Norton, 1994). At the age determined by the experimental protocol (typically at 10 DVE or 21 DVE), each animal was anesthetized (ketamine 17.5 mg; xylazine 1.2 mg, supplemented with 0.5% to 2.0% isoflurane as needed) and received the dental acrylic pedestal.

Refractive Measurements

To assess whether eyes were developing normally or if they were developing an induced myopia or hyperopia, non-cycloplegic refractive measurements were taken with a Nidek autorefractor in non-sedated animals on a schedule that depended on the treatment of the animal. Some were measured each day, while others were measured before treatment and on the last day of treatment.

A-Scan Measurements

A-scan ultrasonographic measures were performed under anesthesia (17.5 mg/kg ketamine HCl with 1.2 mg/kg xylazine, i.m.). While anesthetized, the head of each animal was positioned so that the cornea was perpendicular to the measuring A-scan probe. The heart rate was constantly monitored with an audiomonitor and the tear film was maintained through periodic application of artificial tears (Liquifilm Forte, Allergan) (Norton and McBrien, 1992).

A 15 MHz 6.35 mm ultrasound transducer focused at 20 mm powered by a Panametrics 5052 pulser/receiver was used for the A-scan measures. A 14 mm standoff filled with 0.9% saline provided coupling of the pulser/receiver to the cornea, which was anesthetized with 0.5% Proparacaine hydrochloride solution (Bausch and Lomb). Returning echoes from the intraocular surfaces were first passed through a preamplifier (Accu-Tron Inc., Model 3080) followed by a Tektronix 7603 oscilloscope with a 7D20 digitizer plug-in. Pulses were produced at approximately 5000/sec. The signal-to-noise ratio was enhanced by averaging eight waveforms. Six of the averaged waveforms were collected per eye, stored on a computer, and analyzed using a waveform analysis package (TAMS,

Tektronix Inc.) (Norton and McBrien, 1992). The measurements between ocular surfaces were made to a precision of 0.025 μs and the conversion of time to distance used the previously published conduction velocity values for anterior segment of 1557.5 m/sec, lens conduction velocity of 1723.3 m/sec (Marsh-Tootle and Norton, 1989; Norton and McBrien, 1992), and 1540 m/sec for vitreous (Coleman et al. 1977). These standard conduction velocities were used to convert echo times to distances.

Four components were measured with the A-scan system: anterior segment depth (cornea plus anterior chamber), lens thickness, vitreous chamber depth (measured to the front of the retina), and axial length, which was the sum of the three ocular component dimensions.

TAMS (Tektronix Inc.) was used to analyze the A-scan waveforms. This software package gave the operator the ability to measure the anterior segment depth, lens thickness, vitreous chamber depth, and axial length. This program contained cursors that could be moved by the operator to find the waveform peaks (Figure 5). After each eye was analyzed using the TAMS software, the conduction velocities were used to convert time measurements into distance measurement.

Lenstar Measurements

Lenstar optical biometric measurements were made in un-sedated animals while the animal was gently restrained on a plastic stand in front of the instrument. The Lenstar was focused and aligned using the image of the eye on a monitor. Sixteen waveforms were averaged and a total of three averaged waveforms were collected automatically by the machine. Only those averages that had clear peaks at each ocular surface were kept. A

total of seven components (cornea, anterior chamber, lens, vitreous, retina, choroid, and axial length) were measured using analysis software (Haag-Streit EyeSuite).

To obtain measures of the ocular components from tree shrew eyes, the operator had to confirm that the software had placed a series of cursors in the correct location, or move the cursors to the appropriate location (Figure 8). Because the Lenstar system was designed for human eye measurements, many of the six cursors had to be manually adjusted for tree shrew eyes. The software provided measurements between cursors with the following resolution: corneal thickness (0.001 mm), anterior chamber depth (0.01 mm), lens thickness (0.01 mm), axial length (0.01 mm), retinal thickness (0.001 mm), and choroidal thickness (0.001 mm). Because the Lenstar measures more components than A-scan, some measurements made by the Lenstar were combined in order to be comparable with the A-scans measurements. These components were the corneal thickness and anterior chamber depth which combine to be the anterior segment depth. The EyeSuite software does not provide a direct measurement of vitreous chamber depth. This was calculated by subtracting the corneal thickness, anterior chamber depth, lens thickness, and retinal thickness from the axial length value provided by the software. As will be described in the Results, the vitreous chamber depth values obtained by subtracting the other components from the overall axial length value provided by the software gave numbers that were substantially smaller than those obtained from the A-scan system. It appeared that the Lenstar axial length value is calculated using an average overall human eye refractive index that is inappropriate for tree shrew eyes. It is likely that this difference occurred because the tree shrew crystalline lens is proportionately thicker than the human lens, so the light spends more time in the lens in tree shrew and lens refractive index is

higher than that of other ocular components. To obtain a direct measure of vitreous chamber depth the retinal cursors, which can be moved in the international version of the software, were manually positioned at the posterior lens surface and the front of the retina. Similar values were obtained using the lens cursors, but the retinal cursors provided 3 digits of resolution whereas the lens cursors only provided values to the nearest 0.01 mm.

Data Analysis

Values from the A-scan and Lenstar analyses were entered into an Excel spreadsheet and values for anterior segment, lens thickness, vitreous chamber depth, and axial length were compared. Measurement variability was calculated on 10 randomly selected animals from a pool of all animals. The variability was calculated by taking the variance (VAR). These variances were the VAR of 3 measures made with A-scan and 3 with Lenstar on a single eye, and the average of the individual VARs were calculated. Coefficient of determination values (r^2) were used to evaluate the correlations between the two methods. The method described by Bland and Altman (Altman and Bland, 1986) was employed to determine whether the differences between the A-scan and Lenstar measures varied based on eye size. The Bland-Altman method plots the difference between the measurements from both systems against the average of the measurements for each animal. The 95% limits of agreement were defined as mean ± 1.96 times the standard deviation (SD) of the differences between both systems. A t-test was used to determine significance of the slope for the correlation plots. The cutoff for significance was defined as $p < 0.05$. A t-test was used to determine whether the repeatability for each system using

three waveforms was significantly different. Correction factors were calculated by taking the ratio of the pooled average A-scan component over the Lenstar component.

CHAPTER 3

RESULTS

The ocular component dimensions measured in normal and control eyes with A-scan are provided in Table 1. A-scan measures of the ocular components in treated eyes are provided in Table 2. These are the values against which the Lenstar measures (also listed in Tables 1 and 2) were compared.

The vitreous chamber depth values from the Lenstar in Tables 1 and 2 were made using the retinal cursors. The reason is shown in Figure 10, which compares the vitreous chamber depth obtained by subtracting the other ocular components from the axial length provided by the EyeSuite software (magenta circles) with measures made using the retinal cursors (blue squares). Clearly, the calculated values were much smaller than the measured values. It also was found that if the anterior retinal cursor was moved in the course of measuring retinal thickness, the axial length value provided by the EyeSuite software changed, even though the posterior retinal cursor remained in place. This suggested that the axial length value was calculated in the EyeSuite software using an average human refractive index and was inappropriate for calculating vitreous chamber depth or measuring overall axial length in tree shrew. Vitreous chamber depth measures made with the retinal cursors were used for comparisons between the A-scan and the Lenstar. The axial length values for the Lenstar in Tables 1 and 2 are the sum of the individual ocular components, as was also the case for the A-scan axial length.

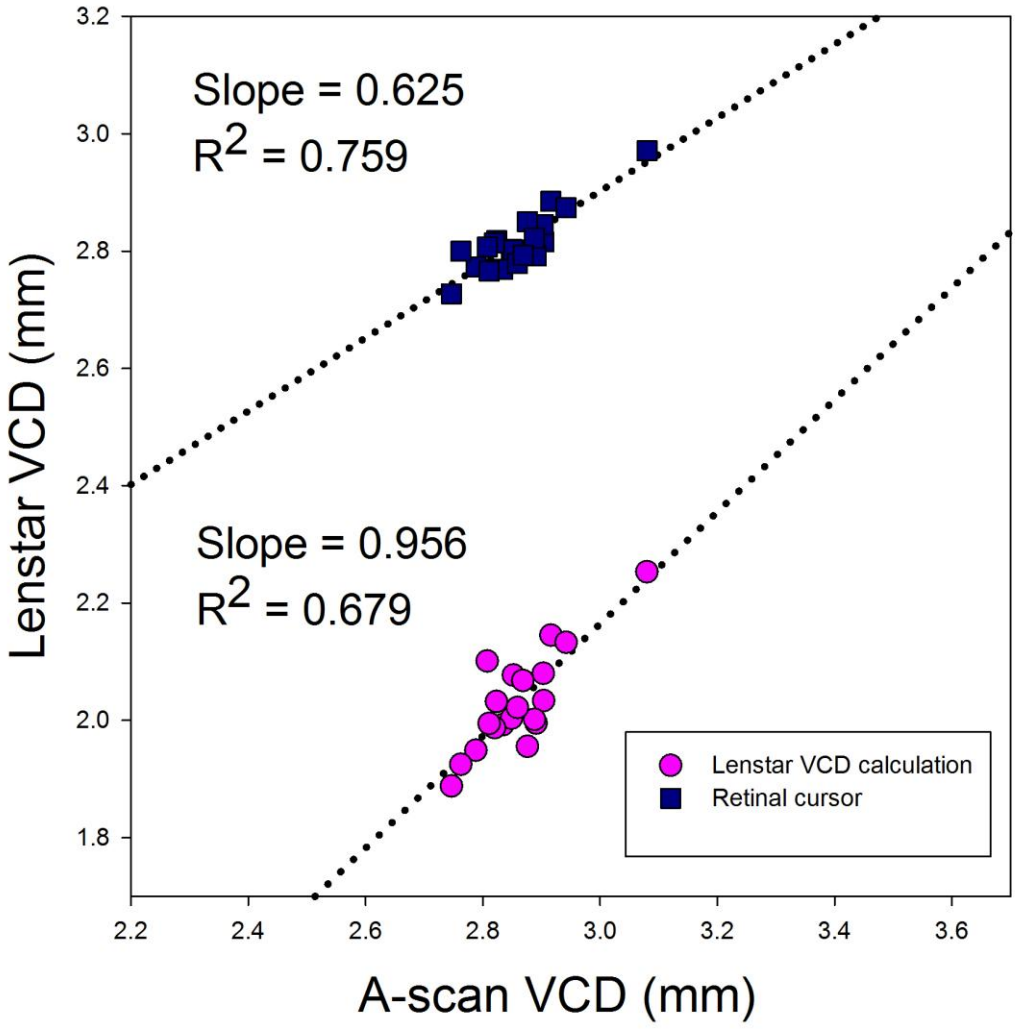

Figure 10. Lenstar LS 900 measures of vitreous chamber depth. Vitreous chamber depth calculated by subtracting ocular components from the axial length provided by the Eye Suite software (magenta circles) and vitreous chamber depth measured using the retinal cursors (blue squares). Comparison shown includes 20 randomly-selected eyes measured using both methods of calculating vitreous chamber depth.

As seen in Tables 1 and 2, the values of the ocular components in the normal and control eyes and in the treated eyes made with the two systems were very similar, but for each component, the Lenstar values were slightly, and significantly, smaller than the A-

scan values. This was true not only for the normal and control eyes, but also for the treated eyes.

Measurement variability was also calculated among the four components (anterior segment depth, lens thickness, vitreous chamber depth, and axial length) using the Lenstar and A-scan system. The variability was calculated by taking the variance (VAR) of 10 randomly selected animals (20 eyes). These variances were the VAR of 3 measures made with A-scan and 3 with Lenstar on a single eye, and the average of the individual VARs were calculated. Anterior segment depth had a variance of 0.020 mm with the A-scan and 0.017 mm with the Lenstar. Lens thickness was found to have a variance of 0.006 mm with the A-scan and 0.014 mm with the Lenstar. Vitreous chamber depth had a variance of 0.002 mm with the A-scan and 0.005 mm with the Lenstar while axial length had a variance of 0.005 mm using the A-scan and 0.004 mm using the Lenstar. The variances between both methods were found to be significantly different for only lens thickness. After looking at the analysis both systems appear to have similar variability between anterior segment depth, vitreous chamber depth, and axial length.

Correction factors were calculated by taking the A-scan measurement/Lenstar measurement for each component. Table 3 lists the correction factors calculated using the pooled data (n=146). It can be noted that the axial length did not need a correction factor after the anterior segment depth, lens thickness, and vitreous chamber depth had been calculated because those components make up the axial length. Following the addition of each factor the system differences were no longer significant.

Table 1

A-scan and Lenstar measurements of anterior segment depth (ASD), lens thickness (LT), vitreous chamber depth (VCD), and axial length (AL) in 86 normal and 30 control eyes.

Component	Method	Average (mm) (mean ± SD)	Difference (mm) (mean ± SD)	Difference (%)	r^2	Slope
ASD	A-scan	0.97 ± 0.05	-0.06 ± 0.04*	6.60	0.49*	0.62
	Lenstar	0.91 ± 0.04				
LT	A-scan	3.18 ± 0.10	-0.08 ± 0.05*	2.48	0.80*	1.07
	Lenstar	3.10 ± 0.12				
VCD	A-scan	2.874 ± 0.06	-0.057 ± 0.028*	2.00	0.77*	0.80
	Lenstar	2.827 ± 0.05				
AL	A-scan	7.03 ± 0.15	-0.20 ± 0.04*	3.06	0.95*	1.10
	Lenstar	6.82 ± 0.17				

* $p < 0.05$

Table 2

A-scan and Lenstar measurements of anterior segment depth (ASD), lens thickness (LT), vitreous chamber depth (VCD), and axial length (AL) in 30 treated eyes.

Component	Method	Average (mm) (mean ± SD)	Difference (mm) (mean ± SD)	Difference (%)	r^2	Slope
ASD	A-scan	1.01 ± 0.05	-0.06 ± 0.03*	5.93	0.56*	0.54
	Lenstar	0.96 ± 0.04				
LT	A-scan	3.43 ± 0.24	-0.04 ± 0.05*	1.29	0.97*	1.04
	Lenstar	3.38 ± 0.25				
VCD	A-scan	2.912 ± 0.16	-0.063 ± 0.03*	2.18	0.96*	0.95
	Lenstar	2.850 ± 0.15				
AL	A-scan	7.36 ± 0.23	-0.19 ± 0.04*	2.55	0.97*	1.01
	Lenstar	7.17 ± 0.24				

* $p < 0.05$

Table 3

Correction factor for Lenstar values

ASD	LT	VCD	AL
1.0655	1.0200	1.0203	N/A

Aim 1: Detailed Comparison Between Systems

Figures 11-14 and the system differences (Lenstar – A-scan) listed in Aim 1 contain the pooled data from the 146 normal, control, and treated eyes. Figure 11A compares the anterior segment values measured with A-scan and Lenstar. The average anterior segment difference (Lenstar minus A-scan) was found to be −0.60 ± 0.04 mm. The Bland-Altman analysis confirmed that the Lenstar measures of anterior segment depth are smaller than those made with A-scan ultrasonography for all eye sizes. The slope of the Bland-Altman plot, −0.13, was not statistically significantly different than zero (Figure 11B). Thus, differences between the two measures did not change as a function of anterior chamber depth. A correction factor of 1.0655 was applied to the pooled data of the anterior segment making the Lenstar not significantly different than the A-scan.

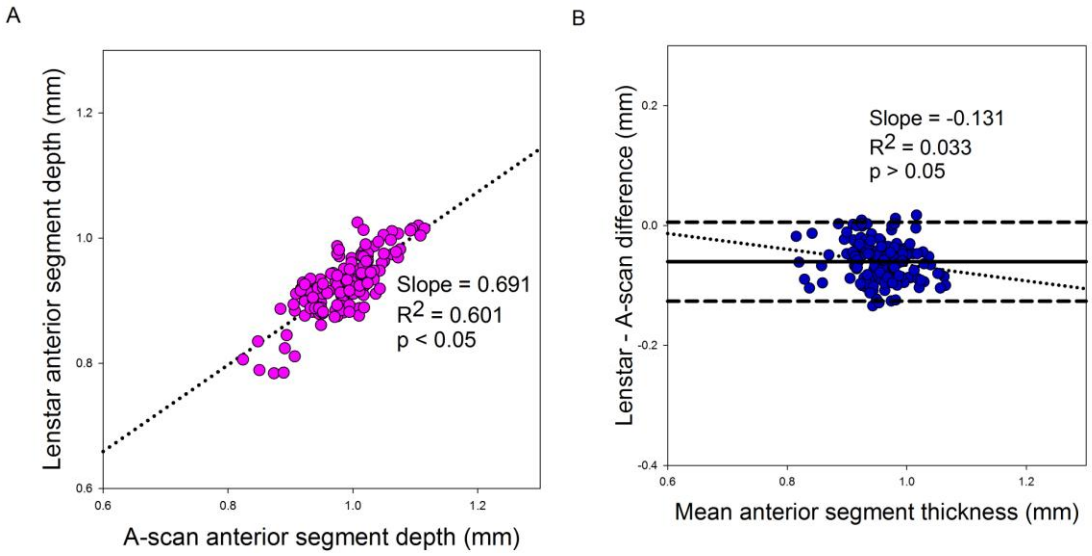

Figure 11. Anterior segment depth measured with A-scan ultrasonography and the Lenstar LS 900. (**A**) Correlation between A-scan and Lenstar. The Lenstar measurements were slightly smaller than the A-scan across all eyes. The larger eyes were those of older animals. The dotted line is the regression. (**B**) Bland-Altman plot. The dotted line is the regression line and shows the slope of the Bland-Altman plot. The dashed lines indicate the 95% limits of agreement. The solid black line is the mean difference (Lenstar minus A-scan).

Figure 12A compares the lens-thickness values made with the A-scan and the Lenstar. On average the lens thickness measured with the Lenstar was smaller than that made with A-scan; the difference was −0.06 ± 0.05 mm. The Bland-Altman analysis (Figure 12B) confirmed that the Lenstar measures of lens thickness are smaller than A-scan and showed that this occurs at all lens thicknesses included in this study. The slope of the Bland-Altman analysis, 0.09, was found to be significantly different than zero indicating that thicker lenses have a smaller Lenstar − A-scan difference than thinner lenses. A correction factor of 1.0200 was applied to the pooled data of the vitreous chamber depth making the Lenstar not significantly different than the A-scan.

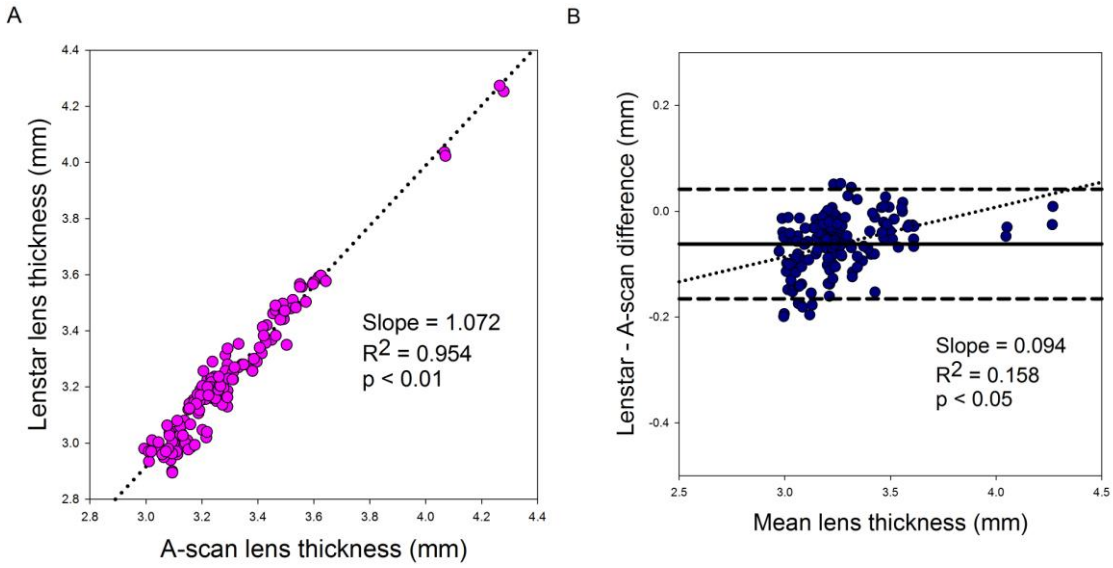

Figure 12. Lens thickness measured with A-scan ultrasonography and the Lenstar LS 900. (**A**) Correlation between A-scan and Lenstar. The Lenstar measurements were slightly smaller than the A-scan across all eyes. The larger eyes were those of older animals. (**B**) Bland-Altman plot. The lens thickness figures had the same line descriptions as listed in Figure 11.

Figure 13A compares the vitreous chamber depth values made with the A-scan and the Lenstar. On average the vitreous chamber depth measured with the Lenstar was smaller than that made with A-scan; the difference was −0.06 ± 0.04 mm. The Bland-Altman plot illustrated that the Lenstar measures of vitreous chamber were smaller than the measures made with A-scan (Figure 13B). The slope of the Bland-Altman, −0.05, was not significant indicating that the difference between the two methods did not change as a function of vitreous chamber depth. A correction factor of 1.0203 was applied to the pooled data of the anterior segment making the Lenstar not significantly different than the A-scan.

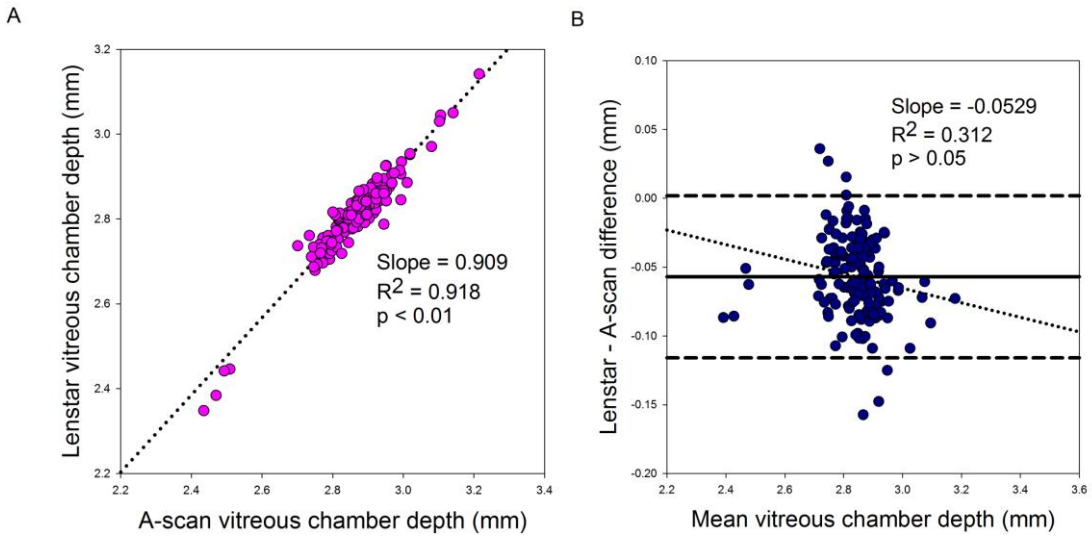

Figure 13. Vitreous chamber depth measured with A-scan ultrasonography and the Lenstar LS 900. (**A**) Correlation between A-scan and Lenstar. The Lenstar measurements were slightly smaller than the A-scan across all eyes. The larger eyes were those of older animals. (**B**) Bland-Altman plot. The vitreous chamber depth figures had the same line descriptions as listed in Figure 11.

Figure 14A compares the axial length values made with the A-scan and the Lenstar. On average the axial length measured with the Lenstar was smaller than that made with A-scan; the difference was −0.20 ± 0.04 mm. The Bland-Altman analysis (Figure 14B) confirmed that the Lenstar measures of axial length are smaller than A-scan. The slope of the Bland-Altman analysis, 0.09, was not significant. Thus, differences between the two methods did not change as a function of axial length. After using the correction factors for the other three components the axial length measured by the Lenstar was no longer significantly different than the A-scan.

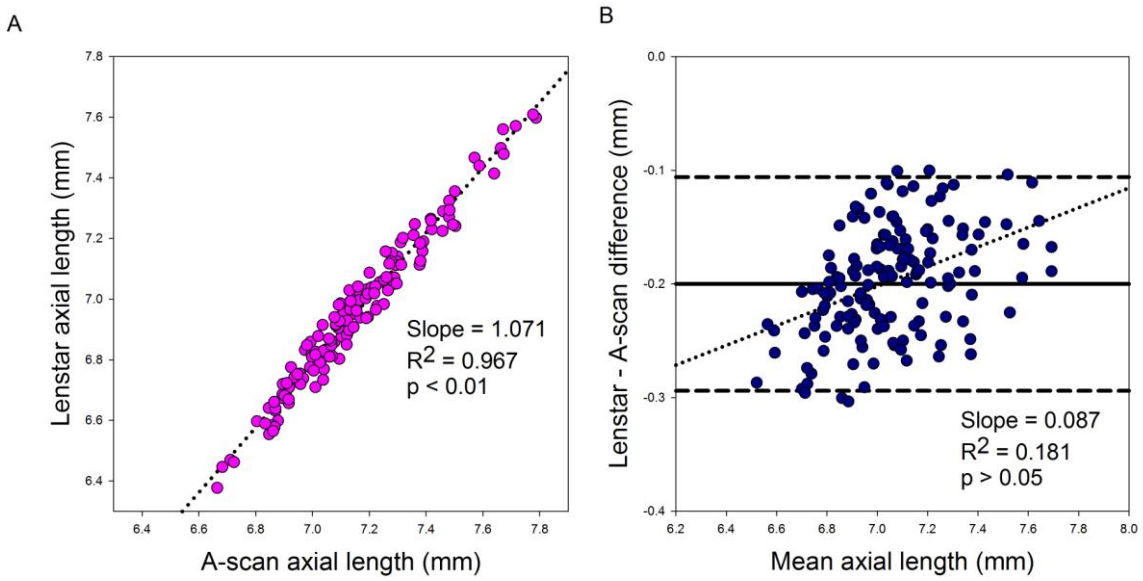

Figure 14. Axial length measured with A-scan ultrasonography and the Lenstar LS 900. (**A**) Correlation between A-scan and Lenstar. The Lenstar measurements were slightly smaller than the A-scan across all eyes. The larger eyes were those of older animals. (**B**) Bland-Altman plot. The axial length figures had the same line descriptions as listed in Figure 11.

Aim 2: Treated – Control Differences

The second aim of the study was to examine differences between treated (myopic or hyperopic) eyes and their fellow untreated control eyes to learn whether the Lenstar provides a similar measure to the A-scan. Ocular component differences between systems are listed in Figures 15 &16; they consist of data from 30 animals in which one eye had received treatment while the other was a control. Table 4 consists solely of data from 24 minus lens animals. When the two systems were compared using only the animals that wore a minus lens vitreous chamber depth and axial length were significantly larger in the treated eyes ($p < 0.05$; Table 4). The average treated − control eye difference between the anterior segment depth was 0.01 ± 0.04 mm with A-scan and 0.01 ± 0.02 with the Lenstar. The Lenstar – A-scan system difference was found to be 0.00 ± 0.02 mm (Table 4). The differences between the treated and control eyes were found to be significantly

correlated on all components except lens thickness using both methods ($p < 0.05$). The system differences (Lenstar vs. A-scan) were not significantly different on any components (Table 4).

Table 4

Comparison of treated minus control eye differences using A-scan ultrasonography and the Lenstar LS900.

Component	System difference (mm) (mean ± SD)	Treatment effect p value	r^2	Slope
ASD	0.00 ± 0.02	> 0.05	0.33*	0.284
LT	0.01 ± 0.03	> 0.05	0.09	0.143
VCD	−0.011 ± 0.03	< 0.05	0.97*	0.962
AL	−0.013 ± 0.05	< 0.05	0.91*	0.955

* $p < 0.05$

The average treated − control eye lens thickness difference was −0.01 ± 0.04 mm for A-scan and −0.01 ± 0.04 mm for the Lenstar. The Lenstar – A-scan system difference was found to be 0.01 ± 0.03 mm (Table 4). Lens thickness did not change in treated eyes.

Vitreous chamber depth was significantly larger in minus lens treated animals. The mean value for treated – control eye vitreous chamber depth differences was 0.110 ± 0.12 mm for A-scan and 0.097 ± 0.12 mm for the Lenstar. The Lenstar – A-scan system difference was −0.011 ± 0.03 mm (Table 4). The Bland-Altman analysis (Figure 15B) confirmed that the Lenstar measures of vitreous chamber depth difference are slightly smaller than A-scan. The slope of the Bland-Altman analysis, −0.05, was not significant. The difference between the two methods did not change as a function of vitreous chamber depth.

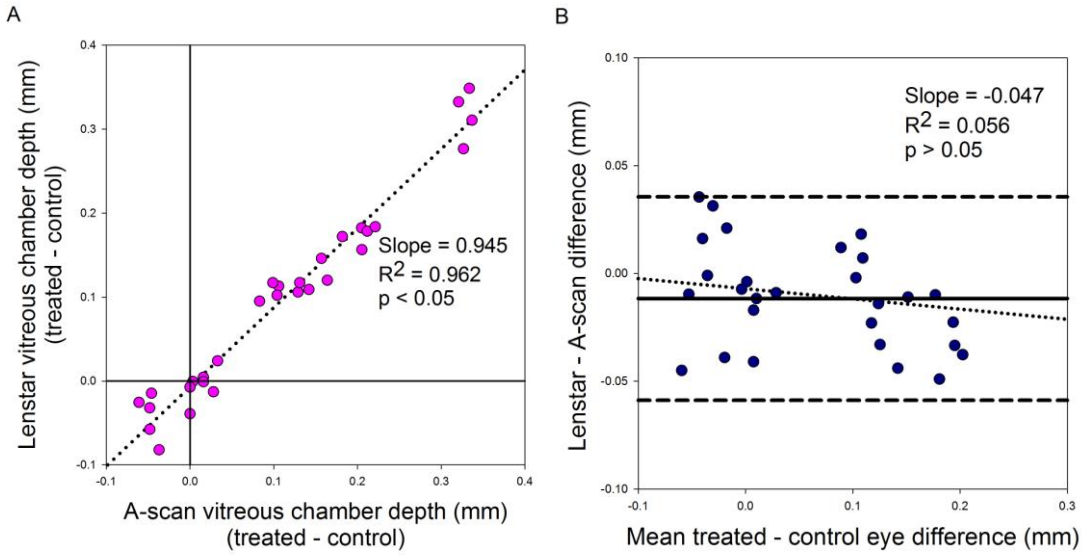

Figure 15. Treated minus control eye difference in vitreous chamber depth measured using A-scan ultrasonography and the Lenstar LS 900. (**A**) There was a high correlation between the treated vs. control eye difference measures with the two methods. (**B**) Bland-Altman plot. The vitreous chamber depth figures had the same line descriptions as listed in Figure 11.

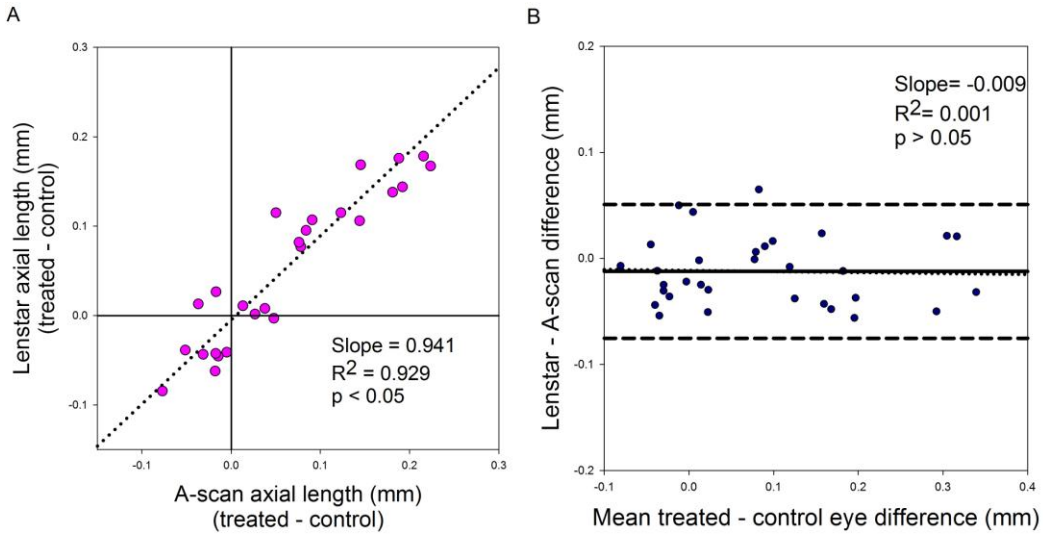

Figure 16. Treated minus control eye difference in axial length measured using A-scan ultrasonography and the Lenstar LS 900. (**A**) There was a high correlation between the treated vs. control eye difference measures with the two methods. (**B**) Bland-Altman plot. The axial length figures had the same line descriptions as listed in Figure 11.

Because of the vitreous chamber depth in minus lens treated animals the average treated − control eye difference between the axial length was 0.10 ± 0.12 mm with A-scan and 0.09 ± 0.12 with the Lenstar. There was a small Lenstar – A-scan system difference, −0.013 ± 0.05 mm (Table 4). The slope of the Bland-Altman analysis, 0.03, was not significant (Figure 16B). The difference between the two methods did not change as a function of axial length.

Vitreous chamber depth differences were plotted against refractive error differences for both systems (Figure 17), including only treated and control eyes. The difference in vitreous chamber depth per diopter difference was 27.2 μm/D for A-scan and 26.1 μm/D for Lenstar. A-scan vitreous chamber differences versus refractive error differences showed a significantly high correlation ($r^2 = 0.96$; $p < 0.05$). Similar to the A-scan, the Lenstar vitreous chamber differences vs. refractive error differences showed a significant correlation ($r^2 = 0.95$; $p < 0.05$). The Lenstar plot also had additional plus lens treated animals to show that the Lenstar could accurately measure myopic shifts as well as hyperopic shifts.

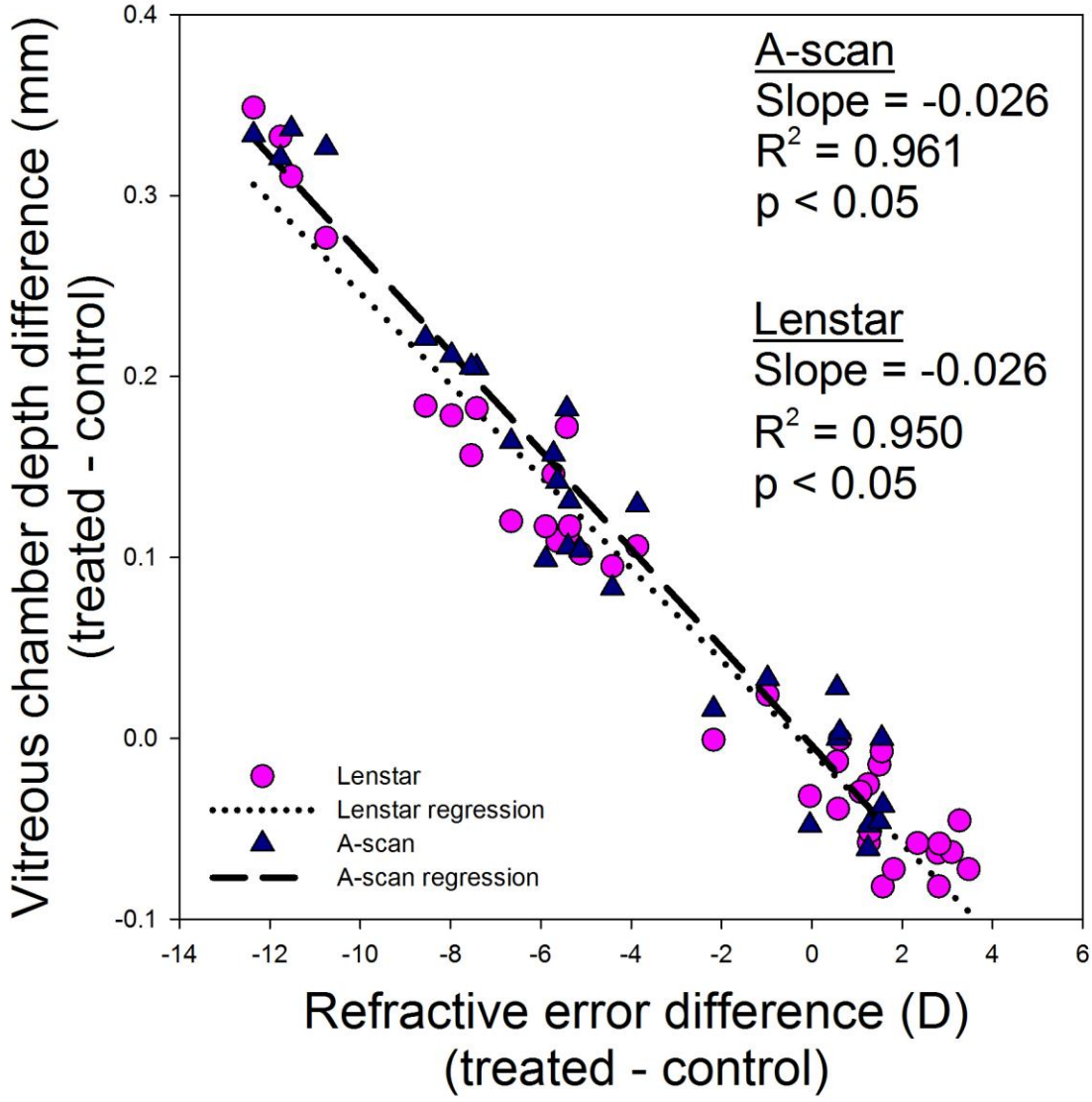

Figure 17. Plots of refractive error difference (treated − control) vs. vitreous chamber depth difference (treated − control) for A-scan and Lenstar. There was a high correlation between refractive error difference and vitreous chamber depth difference for both A-scan ultrasonography and Lenstar and the slopes were very similar. The slopes between the two systems were not significant.

CHAPTER 4

DISCUSSION

A-scan ultrasonography has been a well-established optical component analysis technique in tree shrew myopia studies for many years. The accuracy of the A-scan was tested in the Marsh-Tootle and Norton paper (1989). A-scan ultrasonography was compared to frozen sections of the tree shrew eye. The mean axial lengths for experimental and normal eyes were compared between the A-scan measurements of axial length compared to those measured with the frozen sections (Marsh-Tootle and Norton, 1989). A-scan ultrasonography measured the treated axial length as 8.07 ± 0.14 mm and the control eye as 7.74 ± 0.10 mm. The frozen sections were 8.27 ± 0.23 mm while the control was 7.92 ± 0.13 mm. Sherman et al. (1977) used a micrometer to measure axial length in treated and control eyes. They found that in each case, the deprived eye was longer than the control eye. Axial length values were very similar between both the Marsh-Tootle and Norton paper (1989) and the Sherman et al. paper (1977). The deprived (treated) axial length was 8.13 ± 0.17 mm for the Sherman article compared 8.07 ± 0.14 mm for the Marsh-Tootle and Norton paper. The open (control) axial length was 7.76 ± 0.03 mm for the Sherman article (1977) and 7.74 ± 0.10 mm for the Marsh-Tootle and Norton paper (1989).

The comparison between A-scan ultrasonography and the Lenstar optical biometer was performed in the present study to determine if the newer technology,

Lenstar, could be used in place of the A-scan. This is the first comparison between these two systems in tree shrews. The vitreous chamber depth, calculated from the standard Lenstar cursors, substantially underestimated vitreous chamber depth when compared to the A-scan measures. Using retinal (or even lens) cursors to measure vitreous chamber depth provided much more comparable results.

As expected, because both tools measured the same eyes, the measures of all components were significantly correlated with these two systems. More importantly, a small consistent offset was also found in all the component measurements between the two systems such that the Lenstar values were slightly smaller than the A-scan values.

Analysis of the treated minus control differences led to a significant treatment effect, for myopic eyes, in the vitreous chamber depth and axial length. This was expected because the vitreous chamber depth is what primarily increases when an eye receives minus lens treatment and the vitreous chamber is included in the axial length calculation. The anterior segment depth and lens thickness did not change in minus lens animals as found in previous studies (Marsh-Tootle and Norton, 1989; Siegwart and Norton, 1998).

Overall, measuring the eyes with both the A-scan and Lenstar systems appears to give a small consistent offset in measurements. When both methods were compared, the Lenstar consistently measured a smaller component than the standard system, A-scan ultrasonography. The Lenstar system is calibrated for human eyes only while the A-scan system in the lab is currently calibrate for tree shrew eyes. The Lenstar has been used on human patients to determine the correct intraocular lens. This comparison between systems had a few limitations. The correction factors calculated for the tree shrew eyes do not apply to animals with smaller and larger eyes however the ratio (A-scan/Lenstar)

could still be used to calculate a set of correction factors for certain eye sizes. This analysis was also performed on animals that had system measurements up to three days apart. A follow-up study could be performed where both A-scan and Lenstar were used during the same measurement session. However, a tree shrew eye even at three days between measurements would not change greatly. Anterior segment depth, lens thickness, and axial length should not change much at all while the vitreous chamber depth on average would not grow more than 10 μm.

The results in Aim 1 and Aim 2 support the very strong similarities between the measures made with the two systems. They both appear to give similar values on all four components and both appear to have similar offsets in the components that change when the eye is treated with minus and plus lenses. Therefore it appears that the Lenstar optical biometer can be used in place of A-scan ultrasonography to measure the ocular components of tree shrew eyes. This would make ocular component scans easier because the animals would not need to be anesthetized and scans each day can be performed.

Similar studies have been done that compare ultrasonography with optical biometers in the human population. Cruysberg et al. (2009) found the Lenstar had small but significant differences between the Visante AS-OCT and the IOL Master among ACD and AL. It was concluded that these machines could not be used interchangeably. A pediatric population was tested with the Lenstar and ultrasound biometry. Gursoy et al. (2009) found statistically significant differences in all parameters between the Lenstar and the A-scan, in the pediatric population. However, all the parameters obtained by the Lenstar and the contact devices were significantly correlated with each other. For cataractus eyes in the human population, a significant correlation between anterior cham-

ber depth, lens thickness, and axial length was found between the Lenstar and contact ultrasound biometer (Tomey-AL 3000) (Tappeiner, 2010).

Very few studies have been conducted comparing these systems and none of them have been performed in tree shrews. Compared with the human studies, similar results were found while the Lenstar showed less deviation from our measurements in tree shrew. Human use appears to find that given a significant correlation yet a significant difference, interchangeability is not possible. A similar comparison was done in chicks and showed a similar conclusion with anterior segment depth, vitreous chamber depth, and axial length (Penha et al., 2012). Both found significant correlations between ASD, VCD, and AL. With chicks, more research is needed to determine if the two systems could be used interchangeably. Changes in ocular dimensions induced by treatment was easily resolved and very similar between the two systems. Perhaps given the refractive indices of the ocular components, one could provide a more accurate measurement compared to A-scan. Given technological advances in optical measurement, both systems represent powerful improvements with the Lenstar being a recent alternative to A-scan ultrasonography. If the adjustment factors are applied consistently to all measurements done by the Lenstar, then the Lenstar and A-scan give analogous measurements**.**

REFERENCES

Altman, D.G. & Bland, J. M. Comparison of methods of measuring blood pressure. J Epidemiol Community Health 1986;40:274-277.

Amedo, A. & Norton, T. T. Visual guidance of recovery from lens-induced myopia in tree shrews (*Tupaia glis belangeri*). Ophthalmic Physiol Opt. 2012;32(2): 89–99

Burton, T. C. The influence of refractive error and lattice degeneration on the incidence of retinal detachment. *Trans Am Ophthalmol Soc*. 1989; 87: 143–157

Campbell, C. B. G. The relationships of the tree shrews: the evidence of the nervous system. *Evolution* 1966;20, 276-281.

Coleman, D. Lizzi, F. Jack, R. Ultrasonography of the eye and orbit. London : Henry Kimpton Publishers;1977.

Cruysberg, L. Doors, M. and Verbakel, F. Evaluation of the Lenstar LS 900 non-contact biometer. *British Journal of Ophthalmology* 2010;94, 106-110.

Curtin, B. J. The prevalence of myopia. In *The Myopias - Basic Science and Clinical Management 1985;*Philadelphia: Harper & Row.

Fledelius, H. C. Myopia prevalence in Scandinavia. A survey, with emphasis on factors of relevance for epidemiological refraction studies in general. *Acta Ophthalmol Suppl* 1988;185, 44-50.

Goh, W. S. H. & Lam, C. S. Y. Changes in refractive trends and optical components of Hong Kong Chinese aged 19-39 years. *Ophthalmic Physiol Opt* 1994;14, 378-382.

Gursoy, H., Sahin, A., Basmak, H., Ozer, A., Yildirim, N., and Colak, E. Lenstar Versus Ultrasound for ocular biometry in a pediatric population. *Optometry and Vision Science* 2011;88, 912-919.

Marsh-Tootle, W. L. & Norton, T. T. Refractive and structural measures of lid-suture myopia in tree shrew. *Invest Ophthalmol Vis Sci* 1989;30, 2245-2257.

McBrien, N. A. & Norton, T. T. The development of experimental myopia and ocular component dimensions in monocularly lid-sutured tree shrews (*Tupaia belangeri*). *Vision Res* 1992;32, 843-852.

Norton, T. T. & McBrien, N. A. Normal development of refractive state and ocular component dimensions in the tree shrew (*Tupaia belangeri*). *Vision Res* 1992;32, 833-842.

Norton, T. T., Amedo, A., and Siegwart, J. The effect of age on compensation for a negative lens and recovery from lens-induced myopia in tree shrews (*Tupia glis belangeri*). *Vision Res* 2010;50, 564-576.

Puliafito, C. Hee, M. Schuman, J. and Fujimoto, J. *Optical coherence tomography of optical diseases* 1996;SLACK Incorporated,Thorofare, NJ, 374 p.

Rohrer K, Frueh B, Walti R, Clemetson I, Tappeiner C, Goldblum D. Comparison and evaluation of ocular biometry using a new noncontact optical low-coherence reflectometer. *Ophthalmology* 2009;116: 2087-2092.

Sheedy, J. E. What is the role of glasses in optometry? *Optom Educ.* 1996;21:111-113.

Sherman, S. M. Norton, T. T. & Casagrande, V. A. Myopia in the lid-sutured tree shrew (*Tupaia glis*). *Brain Res* 1977;124, 154-157.

Siegwart, J. T. & Norton, T. T. Refractive and ocular changes in tree shrews raised with plus or minus lenses. *Invest Ophthalmol Vis Sci* 1993;*34, ARVO Abstract S1208*.

Siegwart, J. T. & Norton, T. T. Goggles for controlling the visual environment of small animals. *Lab Animal Sci* 1994;44, 292-294.

Siegwart, J. T. Jr. & Norton, T. T. The susceptible period for deprivation-induced myopia in tree shrew. *Vision Res* 1998;38, 3505-3515.

Siegwart, J. T. Jr. & Norton, T. T. Binocular lens treatment in tree shrews: effect of age and comparison of plus lens wear with recovery from minus lens-induced myopia. *Exp Eye Res* 2010;91, 660-669.

Tappeiner, C. Rohrer, K. Freuh, B. E. Waelti, R. Goldblum, D. Clinical comparison of biometry using the non-contact optical low-coherence reflectometer (Lenstar LS 900) and contact ultrasound biometer (Tomey AL-3000) in cataract eyes. *British Journal of Ophthalmology* 2010;93:949-953

Vitale, S. Ellwein, L. Cotch, M. F. Ferris, F. L. III & Sperduto, R. Prevalence of refractive error in the United States, 1999-2004. *Arch Ophthalmol* 2009;126, 1111-1119.

Wallman, J. & Adams, J. I. Developmental aspects of experimental myopia in chicks: Susceptibility, recovery and relation to emmetropization. *Vision Res* 1987;27, 1139-1163.

Wallman, J. Turkel, J. & Trachtman, J. Extreme myopia produced by modest change in early visual experience. *Science* 1978;201, 1249-1251.

Wiesel, T. N. & Raviola, E. Myopia and eye enlargement after neonatal lid fusion in monkeys. *Nature* 1977;266, 66-68.

APPENDIX

IACUC APPROVAL

THE UNIVERSITY OF ALABAMA AT BIRMINGHAM

Institutional Animal Care and Use Committee (IACUC)

NOTICE OF APPROVAL

DATE: March 18, 2013

TO: THOMAS T NORTON, Ph.D.
WORB-606
(205) 934-6742

FROM:

Robert A. Kesterson, Ph.D., Chair
Institutional Animal Care and Use Committee (IACUC)

SUBJECT: Title: Mechanisms of Ocular Development
Sponsor: NIH
Animal Project_Number: 130208727

As of February 23, 2013 the animal use proposed in the above referenced application is approved. The University of Alabama at Birmingham Institutional Animal Care and Use Committee (IACUC) approves the use of the following species and number of animals:

Species	Use Category	Number In Category
Tree Shrews	A	50
Tree Shrews	B	100

Animal use must be renewed by February 22, 2014. Approval from the IACUC must be obtained before implementing any changes or modifications in the approved animal use.

Please keep this record for your files, and forward the attached letter to the appropriate granting agency.

Refer to Animal Protocol Number (APN) 130208727 when ordering animals or in any correspondence with the IACUC or Animal Resources Program (ARP) offices regarding this study. If you have concerns or questions regarding this notice, please call the IACUC office at (205) 934-7692.

Institutional Animal Care and Use Committee (IACUC)
CH19 Suite 403
933 19th Street South
(205) 934-7692
FAX (205) 934-1188

Mailing Address:
CH19 Suite 403
1530 3rd Ave S
Birmingham, AL 35294-0019

THE UNIVERSITY OF ALABAMA AT BIRMINGHAM

Institutional Animal Care and Use Committee (IACUC)

MEMORANDUM

DATE: March 18, 2013

TO: THOMAS T NORTON, Ph.D.
WORB-606
(205) 934-6742

FROM: 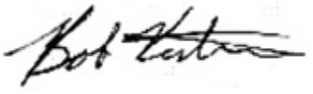

Robert A. Kesterson, Ph.D., Chair
Institutional Animal Care and Use Committee (IACUC)

SUBJECT: **NOTICE OF APPROVAL - Please forward this notice to the appropriate granting agency.**

The following application was renewed by the University of Alabama at Birmingham Institutional Animal Care and Use Committee (IACUC) on February 22, 2013.

Title: Mechanisms of Ocular Development
Sponsor: NIH

This institution has an Animal Welfare Assurance on file with the Office of Laboratory Animal Welfare (OLAW), is registered as a Research Facility with the USDA, and is accredited by the Association for Assessment and Accreditation of Laboratory Animal Care International (AAALAC).

Institutional Animal Care and Use Committee (IACUC)
CH19 Suite 403
933 19th Street South
(205) 934-7692
FAX (205) 934-1188

Mailing Address:
CH19 Suite 403
1530 3rd Ave S
Birmingham, AL 35294-0019

UAB SCHOOL OF OPTOMETRY

Department of Vision Sciences

January 3, 2013

OK per Dr. Engel

To: UAB Graduate School

From: Dr. Thomas T. Norton, Professor

Subject: Animal approval for Mr. Drew Gann

Mr. Gann is advancing to candidacy in the Master's Program in Biology completing research in my lab. The lab is approved to make non-invasive measures of ocular component dimensions (the size of various parts of the eye) using A-scan ultrasound and also an optical biometer (Lenstar, Haag-Streit). Mr. Gann's thesis project is to compare these two measures using data that are collected by other members of the lab who are listed on our IACUC approval.

Mr. Gann has no direct contact with the animals, has therefore not received training on handling our research animal, tree shrew, and is not listed on our protocol. Mr. David Cannon, IACUC Director, suggested in a conversation today that Mr. Gann did not need to be added to the protocol and that this memo, along with a copy of our IACUC approval, should be sufficient to allow him to advance to candidacy.

Thomas T. Norton, Ph.D.

636 Worrell Building
924 18th Street South
205.934.0568
Fax 205.934.5725
visionsciences@uab.edu

The University of
Alabama at Birmingham
Mailing Address:
WORB 636
1530 3RD AVE S
BIRMINGHAM AL 35294-4390